
Directional Ensemble Aggregation for Actor-Critics

Nicklas Werge* Yi-Shan Wu Bahareh Tasdighi Melih Kandemir

Department of Mathematics and Computer Science
University of Southern Denmark

Abstract

Off-policy reinforcement learning in continuous control tasks depends critically on accurate Q -value estimates. Conservative aggregation over ensembles, such as taking the minimum, is commonly used to mitigate overestimation bias. However, these static rules are coarse, discard valuable information from the ensemble, and cannot adapt to task-specific needs or different learning regimes. We propose Directional Ensemble Aggregation (DEA), an aggregation method that adaptively combines Q -value estimates in actor-critic frameworks. DEA introduces two fully learnable directional parameters: one that modulates critic-side conservatism and another that guides actor-side policy exploration. Both parameters are learned using ensemble disagreement-weighted Bellman errors, which weight each sample solely by the direction of its Bellman error. This directional learning mechanism allows DEA to adjust conservatism and exploration in a data-driven way, adapting aggregation to both uncertainty levels and the phase of training. We evaluate DEA across continuous control benchmarks and learning regimes — from interactive to sample-efficient — and demonstrate its effectiveness over static ensemble strategies.

1 Introduction

Off-policy reinforcement learning (RL) has become a powerful framework for solving continuous control tasks, with actor-critic methods forming a central class of algorithms [23, 24]. These methods decompose training into two components: a *critic* (Q -function), which estimates the expected returns, and an *actor*, which uses these Q -value estimates to optimize its policy [14]. Therefore, the accuracy of the Q -function is critical.

A central challenge in actor-critic methods is *overestimation bias* in Q -value estimation [37], which can lead to unstable training and suboptimal policies [40, 41]. This issue is especially problematic in continuous control, where even small biases in Q -values can be exploited by the actor and accumulate over the course of training. Another key challenge is *sample efficiency*. A common strategy to improve it is to increase the number of updates per environment interaction — defined as the update-to-data (UTD) ratio. However, higher UTD ratios place additional demands on the accuracy of Q -value estimates, as more updates per environment interaction can amplify existing biases and further destabilize training [29].

To mitigate overestimation, many algorithms use ensemble critics and aggregate their outputs conservatively — typically by taking the minimum across the ensemble [10–12, 14]. While effective at bias reduction, these static aggregation rules have several limitations. First, they impose unnecessary restrictions that prevent smooth interpolation between conservatism and optimism, hindering nuanced control over the exploration-exploitation trade-off. Second, they discard useful information by collapsing ensemble outputs into a single value. Third, static rules are fixed throughout training and cannot adapt to task-specific needs or the evolving reliability of Q -value estimates across different

*Corresponding author: werge@sdu.dk.

learning stages/tasks. This rigidity also extends to policy optimization, where the actor relies on the same static aggregation — regardless of the exploration demands of the environment or the stage of training.

Furthermore, most algorithms are designed with a specific *learning regime* — defined by particular combinations of UTD ratios and ensemble sizes — in mind. For example, *interactive learning* typically employs low UTD ratios and smaller ensembles with frequent environment interactions [11, 12, 14, 25]. Conversely, *sample-efficient learning* relies on higher UTD ratios and larger ensembles to minimize the number of interactions required to learn a task [8, 10, 43]. Algorithms tailored to a specific learning regime often struggle when applied beyond their intended setting: increasing the UTD ratio in methods designed for interactive learning can introduce instability and degrade performance [29], whereas methods optimized for sample-efficient learning tend to underperform in low-UTD scenarios due to insufficient utilization of available updates [10, 21].

Our approach We propose Directional Ensemble Aggregation (DEA), an adaptive method for Q -value aggregation in actor-critics. DEA addresses two key limitations of existing ensemble-based actor-critic methods: (i) they rely on static aggregation rules — such as taking the minimum or the mean — that remain fixed throughout training and cannot adjust to changing task demands or uncertainty levels; and (ii) this staticness makes them inherently specialized to specific learning regimes, limiting their applicability and generalization beyond those settings.

DEA introduces a fully learnable aggregation strategy that adapts dynamically in a data-driven manner, adjusting its behavior based on task uncertainty, the phase of training, and the underlying learning regime. A central feature is its decoupled aggregation mechanism, which independently controls the aggregation used by the critic and the actor. This design allows the critic to remain conservative under high uncertainty — mitigating overestimation bias — while enabling the actor to favor optimistic estimates when uncertainty is low, thereby encouraging exploration.

To achieve this, DEA learns two directional aggregation parameters during training: one for the critic ($\bar{\kappa}$) and one for the actor (κ). These parameters are learned directly from data via a two-stage Bellman objective weighted by ensemble disagreement, where only the direction of each sample’s Bellmann error affects the update. This directional update scheme enables DEA to adapt its aggregation strategy according to the reliability of the Q -value estimates.

In practice, DEA remains stable in interactive regimes (with low UTD ratios and small ensembles) and performs effectively in sample-efficient settings (with high UTD ratios and large ensembles). Across a broad range of continuous control tasks, DEA consistently demonstrates reliable learning dynamics, highlighting the importance of directional, uncertainty-aware aggregation in actor-critics.

Organization Section 2 introduces background and notation. Section 3 formalizes the soft actor-critic framework, followed by a review of static ensemble aggregation methods in Section 4. Section 5 presents our proposed method, DEA, detailing its directional aggregation mechanism and learning procedure. Empirical results across various control tasks and learning regimes are reported in Section 6, with further analysis in Section 7. We discuss related work in Section 8 and conclude with limitations and future directions in Section 9.

2 Preliminary

We denote by $\mathcal{P}(\Omega)$ the set of all probability distributions over a space Ω , and by $\mathcal{B}(\Omega)$ the set of bounded real-valued functions on Ω . For $N \in \mathbb{N}$, we write $[N]$ for $\{1, \dots, N\}$.

Markov decision processes (MDPs) We consider an infinite-horizon Markov decision process defined by the tuple $\mathcal{M} = \langle \mathcal{S}, \mathcal{A}, p, p_0, r, \gamma \rangle$ [32], where \mathcal{S} and \mathcal{A} are continuous state and action spaces. The transition dynamics are governed by an unknown probability density $p(s'|s, a)$ over next states $s' \in \mathcal{S}$ given a current state-action pair $(s, a) \in \mathcal{S} \times \mathcal{A}$. The initial state is drawn from a distribution $p_0 \in \mathcal{P}(\mathcal{S})$, and rewards are given by a bounded function $r : \mathcal{S} \times \mathcal{A} \rightarrow [0, B_r]$, with $B_r > 0$. The discount factor $\gamma \in (0, 1]$ controls the importance of future rewards.

Policies Let $\Pi = \{\pi : \mathcal{S} \rightarrow \mathcal{P}(\mathcal{A})\}$ denote the set of stochastic policies. Under a policy $\pi \in \Pi$, the agent interacts with the MDP iteratively: at each time step $t \in \mathbb{N}$, the agent observes a state

$s_t \in \mathcal{S}$, samples an action $a_t \sim \pi(\cdot|s_t)$, receives a reward $r(s_t, a_t)$, and transitions to a next state $s_{t+1} \sim p(\cdot|s_t, a_t)$. For convenience, we define the one-step policy-induced transition distribution as $p^\pi(s', a'|s, a) = p(s'|s, a)\pi(a'|s')$.

Maximum entropy RL The objective is to find a policy π that maximizes the expected discounted return, $J(\pi) = \mathbb{E}_\pi[\sum_{t=0}^{\infty} \gamma^t r(s_t, a_t)]$ with $s_0 \sim p_0$ [6, 36]. To encourage exploration, we consider the maximum entropy RL framework [13, 14, 44], where the agent aims to maximize both the expected return and the entropy of the policy. This is formalized by the objective: $J_\alpha(\pi) = \mathbb{E}_\pi[\sum_{t=0}^{\infty} \gamma^t (r(s_t, a_t) + \alpha \mathcal{H}(\pi(\cdot|s_t)))]$, where $\alpha > 0$ controls the trade-off between reward and entropy, and the entropy term is defined as $\mathcal{H}(\pi(\cdot|s)) = -\mathbb{E}_{a \sim \pi(\cdot|s)}[\log \pi(a|s)]$. Haarnoja et al. [15] proposed automatic entropy tuning by adjusting α to minimize the objective $J(\alpha) = \mathbb{E}_{a \sim \pi(\cdot|s)}[\log(\alpha) \cdot (-\log \pi(a|s) - \mathcal{H}_{\text{target}})]$ during each policy update. This objective increases α when the current policy entropy is below the target $\mathcal{H}_{\text{target}}$, and to decrease when it is above. In practice, the target entropy $\mathcal{H}_{\text{target}}$ is typically set heuristically, proportional to $-\dim(\mathcal{A})$ or $-\dim(\mathcal{A})/2$ [10, 15]. The state-action value function $Q^\pi : \mathcal{S} \times \mathcal{A} \rightarrow \mathbb{R}$ under policy π satisfies $Q^\pi(s, a) = J_\alpha(\pi)$ starting from $s_0 = s$ and $a_0 = a$ [13, 42]. It is the unique fixed point of the soft Bellman operator $T^\pi : \mathcal{B}(\mathcal{S} \times \mathcal{A}) \rightarrow \mathcal{B}(\mathcal{S} \times \mathcal{A})$, given by $T^\pi Q(s, a) = r(s, a) + \gamma \mathbb{E}_{(s', a') \sim p^\pi(\cdot|s, a)}[Q(s', a') - \alpha \log \pi(a'|s')]$, so that $T^\pi Q^\pi = Q^\pi$.

3 Soft actor-critic methods

A widely used framework for maximum entropy RL is the class of soft actor-critic methods, where the agent jointly learns a Q -value function (the critic) and a policy (the actor). The active *critic* Q estimates the state-action value function Q^π (following policy π) by minimizing the Bellman error [6, 14, 35]:

$$\arg \min_Q \mathbb{E}_{(s, a, r, s') \sim \mathcal{D}}[(Q(s, a) - y(s, a, r, s'))^2], \quad (1)$$

where the samples (s, a, r, s') are drawn from a replay buffer \mathcal{D} , and the critic's *target value* $y(s, a, r, s')$ is defined as:

$$y(s, a, r, s') = r(s, a) + \gamma[\bar{Q}(s', a') - \alpha \log \pi(a'|s')], \quad a' \sim \pi(\cdot|s'), \quad (2)$$

with \bar{Q} denoting the *target critic* that may differ from the active critic Q [24]. The *actor* is trained to find a policy $\pi \in \Pi$ that maximizes the expected entropy-regularized value:

$$\arg \max_{\pi \in \Pi} \mathbb{E}_{a \sim \pi(\cdot|s)}[\tilde{Q}(s, a) - \alpha \log \pi(a|s)], \quad (3)$$

where \tilde{Q} is a separate *actor-update critic* used solely for training the actor, and may differ from both the active critic Q and the target critic \bar{Q} .

In the idealized setting with exact Bellman policy evaluation, all three value estimators — Q , \bar{Q} , and \tilde{Q} — would match the true value function Q^π [36]. However, different actor-critic methods — such as SAC [14] and REDQ [10] — differ primarily in how they construct the target critic \bar{Q} and the actor-update critic \tilde{Q} from an ensemble.

In Section 4, we review how existing soft actor-critic methods instantiate these components and highlight their limitations. Next, in Section 5, we introduce our proposed DEA approach, which generalizes these constructions through a fully learnable and adaptive ensemble aggregation strategy.

4 Ensemble aggregation in soft actor-critic methods

Ensembles of Q -functions have become standard in modern actor-critic algorithms for improving stability and mitigating overestimation bias. Most methods aggregate the outputs of these critics using conservative rules — typically by taking the minimum across the ensemble — and pair this with delayed copies as target networks to stabilize updates [12, 22, 24]. Formally, for each $i \in [N]$, let $Q_i : \mathcal{S} \times \mathcal{A} \rightarrow \mathbb{R}$ be the (active) critic and $\bar{Q}_i : \mathcal{S} \times \mathcal{A} \rightarrow \mathbb{R}$ its corresponding (delayed) target critic.

The minimum strategy, introduced by Fujimoto et al. [12] and adopted by SAC [14], aggregates the ensemble by selecting the lowest Q -value estimate. SAC employs this rule for both the critic target,

\bar{Q} , used in (2), and the actor-update value, \tilde{Q} , used in (3);

$$\text{SAC:} \quad \bar{Q}(s, a) = \min_{i \in [N]} \bar{Q}_i(s, a) \quad \text{and} \quad \tilde{Q}(s, a) = \min_{i \in [N]} Q_i(s, a).$$

SAC works well for small ensembles (e.g., $N = 2$), but becomes overly conservative as N grows, often leading to underestimation and overly cautious policies [17, 18]. Instead, Chen et al. [10] proposed REDQ, which maintains a larger ensemble of $N = 10$ critics and applies different aggregation strategies for critic and actor. At each critic update, REDQ samples a random subset $S \subset [N]$ of size $|S| = 2$ and uses the minimum over this subset as the target critic, and for actor policy updates it uses the average over the full N -ensemble;

$$\text{REDQ:} \quad \bar{Q}(s, a) = \min_{i \in S} \bar{Q}_i(s, a) \quad \text{and} \quad \tilde{Q}(s, a) = \frac{1}{N} \sum_{i=1}^N Q_i(s, a).$$

This decoupled aggregation balances critic conservatism (via a minimum of a random subset) with actor expressiveness (via a full ensemble average), providing improved training stability and greater sample efficiency compared to SAC, particularly in high UTD ratio regimes.

Limitations SAC and REDQ share structural limitations. Both rely on static aggregation rules for \bar{Q} and \tilde{Q} , which do not generalize well across learning regimes; SAC’s use of a fixed minimum becomes increasingly conservative with larger ensembles, often resulting in persistent underestimation [29]. In contrast, REDQ’s actor-side averaging can become unstable when the ensemble is small.

5 Directional ensemble aggregation in soft actor-critic methods

Directional Ensemble Aggregation (DEA) introduces a fully learnable framework for ensemble-based value estimation in actor-critic methods. It generalizes static aggregation strategies like SAC and REDQ by learning conservative critic targets and an explorative actor in a data-driven manner, enabling adaptation to uncertainty and training dynamics. DEA introduces two scalar parameters: $\bar{\kappa}$, which controls critic-side conservatism, and κ , which modulates actor-side exploration. Both are updated online based on the ensemble’s internal disagreement. An overview of aggregation strategies across methods is provided in Table 1.

Table 1: Aggregation strategies for the target critic (\bar{Q}) and the actor-update critic (\tilde{Q}). $\bar{\delta}$ and δ denote ensemble disagreement for \bar{Q} and \tilde{Q} , respectively, while $\bar{\kappa}$ and κ are DEA’s learnable aggregation parameters for the critic and actor components, respectively.

Method	Target critic \bar{Q}	Actor-update critic \tilde{Q}
SAC	$\min_{i \in [N]} \bar{Q}_i$	$\min_{i \in [N]} Q_i$
REDQ	$\min_{i \in S} \bar{Q}_i$	$\frac{1}{N} \sum_{i=1}^N Q_i$
DEA	$\frac{1}{N} \sum_{i=1}^N \bar{Q}_i + \bar{\kappa} \cdot \bar{\delta}$	$\frac{1}{N} \sum_{i=1}^N Q_i + \kappa \cdot \delta$

DEA integrates seamlessly into the soft actor-critic framework (Section 3); its full update cycle is outlined in Algorithm 1, with the design rationale discussed below.

Ensemble disagreement To quantify the ensemble’s internal uncertainty, DEA uses a measure of ensemble disagreement. Specifically, for a state-action pair (s, a) , we define:

$$\delta(\{Q_i(s, a)\}_{i=1}^N) = \frac{1}{\binom{N}{2}} \sum_{i>j} |Q_i(s, a) - Q_j(s, a)|, \quad \text{for } i, j \in [N].$$

This disagreement metric simply computes the average pairwise absolute difference between Q -value estimates. It is non-parametric, does not rely on distributional critics [5], and can be computed directly from the ensemble’s Q -value predictions. Related notions of ensemble diversity are discussed in more detail in Section 8. For notational clarity, we define $\bar{\delta}(s, a)$ and $\delta(s, a)$ as the disagreement among target critics and active critics, respectively:

$$\bar{\delta}(s, a) \triangleq \delta(\{\bar{Q}_i(s, a)\}_{i=1}^N) \quad \text{and} \quad \delta(s, a) \triangleq \delta(\{Q_i(s, a)\}_{i=1}^N).$$

Soft actor-critic learning with DEA DEA is built on the general soft actor-critic framework (Section 3), but it can seamlessly generalize to other algorithmic families. We chose SAC as a use case, as it is the only commonly adopted algorithm with established variants tailored to the learning

Algorithm 1 Directional Ensemble Aggregation (DEA)

```

1: Initialize: replay buffer  $\mathcal{D} = \emptyset$ ; critic networks  $Q_{\theta_1}, \dots, Q_{\theta_N}$  and actor network  $\pi_\phi$  with random
   parameters  $\{\theta_i\}_{i=1}^N$  and  $\phi$ ; target critic networks  $\bar{Q}_{\bar{\theta}_1}, \dots, \bar{Q}_{\bar{\theta}_N}$  with  $\bar{\theta}_i \leftarrow \theta_i$  for  $i = 1, \dots, N$ 
2: for each environment interaction do
3:   take action  $a_t \sim \pi_\phi(\cdot|s_t)$ , observe reward  $r_t \triangleq r(s_t, a_t)$ , transition to new state  $s_{t+1} \sim p(\cdot|s_t, a_t)$ , and add  $(s_t, a_t, r_t, s_{t+1})$  to replay buffer  $\mathcal{D}$ 
4:   for each update-to-data ratio do
5:     sample mini-batch  $B = \{(s, a, r, s', a') : (s, a, r, s') \sim \mathcal{D}, a' \sim \pi_\phi(\cdot|s')\}$ 
6:      $\theta_i \leftarrow \theta_i - \eta_\theta \nabla_\theta \left\{ \frac{1}{|B|} \sum_B (Q_{\theta_i}(s, a) - y_{\bar{\kappa}})^2 \right\}, \forall i \in [N]$   $\triangleright$  critic
7:      $\bar{\theta}_i \leftarrow \tau \theta_i + (1 - \tau) \bar{\theta}_i, \forall i \in [N]$   $\triangleright$  target critic
8:      $\bar{\kappa} \leftarrow \bar{\kappa} - \eta_{\bar{\kappa}} \nabla_{\bar{\kappa}} \left\{ \frac{1}{|B|} \sum_B |\tilde{Q}_{\bar{\kappa}}(s, a) - y_{\bar{\kappa}}| / \bar{\delta}(s', a') \right\}$   $\triangleright$  target critic DEA parameter
9:      $\kappa \leftarrow \kappa - \eta_\kappa \nabla_\kappa \left\{ \frac{1}{|B|} \sum_B |\tilde{Q}_\kappa(s, a) - y_{\bar{\kappa}}| / \delta(s, a) \right\}$   $\triangleright$  actor DEA parameter
10:     $\phi \leftarrow \phi + \eta_\phi \nabla_\phi \left\{ \frac{1}{|B|} \sum_B (\tilde{Q}_\kappa(s, a_\phi(s)) - \alpha \log \pi_\phi(a_\phi(s)|s)) \right\}, a_\phi(s) \sim \pi_\phi(\cdot|s)$   $\triangleright$  policy
11:     $\alpha \leftarrow \alpha + \eta_\alpha \nabla_\alpha \left\{ \frac{1}{|B|} \sum_B (\log(\alpha) (-\log \pi_\phi(a|s) - \mathcal{H}_{\text{target}})) \right\}$   $\triangleright$  entropy

```

regimes considered in this work. It replaces fixed aggregation with directional, uncertainty-aware versions of the target critic \bar{Q} and the actor-update critic \tilde{Q} :

$$\text{DEA: } \bar{Q}_{\bar{\kappa}}(s, a) = \frac{1}{N} \sum_{i=1}^N \bar{Q}_i(s, a) + \bar{\kappa} \cdot \bar{\delta}(s, a) \quad \text{and} \quad \tilde{Q}_\kappa(s, a) = \frac{1}{N} \sum_{i=1}^N Q_i(s, a) + \kappa \cdot \delta(s, a).$$

Instead of (2), the critic is trained using the modified *target value* using $\bar{Q}_{\bar{\kappa}}$:

$$y_{\bar{\kappa}}(s, a, r, s') = r(s, a) + \gamma [\bar{Q}_{\bar{\kappa}}(s', a') - \alpha \log \pi(a'|s')], \quad a' \sim \pi(\cdot|s'). \quad (4)$$

As in previous work (see e.g., Section 3), DEA ensures stability through delayed target critics, which prevent rapid shifts in the target value signal. Additionally, all critics are trained toward a shared ensemble-based target value (4), promoting consistency across the ensemble and avoiding instability caused by divergent critic objectives.

For policy optimization, the actor is maximizing the entropy-regularized return under the modified *actor-update critic* \tilde{Q}_κ estimate:

$$\arg \max_{\pi \in \Pi} \mathbb{E}_{a \sim \pi(\cdot|s)} [\tilde{Q}_\kappa(s, a) - \alpha \log \pi(a|s)]. \quad (5)$$

Learning the directional aggregation parameters DEA uses a two-stage learning scheme to update $\bar{\kappa}$ and κ , ensuring a directional relationship between critic and actor objectives. The critic-side parameter $\bar{\kappa}$ is optimized to produce stable, conservative targets by minimizing the ensemble disagreement-weighted Bellman error:

$$\arg \min_{\bar{\kappa}} \mathbb{E}_{(s, a, r, s') \sim \mathcal{D}, a' \sim \pi(\cdot|s')} [|\tilde{Q}_\kappa(s, a) - y_{\bar{\kappa}}(s, a, r, s')| / \bar{\delta}(s', a')]. \quad (6)$$

Subsequently, the actor-side parameter κ is updated to track the learned critic target while being regularized by disagreement:

$$\arg \min_{\kappa} \mathbb{E}_{(s, a, r, s') \sim \mathcal{D}, a' \sim \pi(\cdot|s')} [|\tilde{Q}_\kappa(s, a) - y_{\bar{\kappa}}(s, a, r, s')| / \delta(s, a)]. \quad (7)$$

The objectives in (6) and (7) are based on disagreement-weighted absolute errors, which yield sign-based gradients. Specifically, the gradient of (6) with respect to $\bar{\kappa}$ is $-\gamma \mathbb{E}[\text{sign}(\tilde{Q}_\kappa(s, a) - y_{\bar{\kappa}}(s, a, r, s'))]$, and the gradient of (7) with respect to κ is $\mathbb{E}[\text{sign}(\tilde{Q}_\kappa(s, a) - y_{\bar{\kappa}}(s, a, r, s'))]$. These disagreement-weighted losses ensure that each sample contributes equally to the updates of $\bar{\kappa}$ and κ — only the sign of the difference between the critic's prediction and the target value matters. This leads to directional updates that down-weight noisy or uncertain targets, preventing overfitting to high-uncertainty samples. As a result, the updates follow the average direction in the mini-batch, rather than its magnitude. This directional nature is what gives DEA its name: *directional ensemble aggregation*

In practice, due to the entropy term $-\alpha \log \pi(a'|s')$ being positive, the target value $y_{\bar{\kappa}}$ often exceeds the current prediction \tilde{Q}_{κ} . As a result, the error $\tilde{Q}_{\kappa} - y_{\bar{\kappa}}$ is typically negative, which drives $\bar{\kappa}$ lower — leading to more conservative critic targets — and κ higher — encouraging more optimistic/exploratory policy updates for the actor.

Ensemble disagreement and its effect on conservatism and exploration Early in training, limited data and unrefined critics lead to high disagreement across the ensemble. As learning progresses and the critics become more aligned, disagreement tends to decrease — especially relative to the growing scale of the Q -values (e.g., see Figures 6 and 7 in Appendix C). This evolving disagreement plays a key role in regulating the balance between conservatism and exploration in DEA and helps mitigate primacy bias — where early, noisy data disproportionately influences learning — by reducing the weight of unreliable early estimates [29].

The parameter $\bar{\kappa}$ controls the influence of ensemble disagreement $\bar{\delta}$ on the critic target $y_{\bar{\kappa}}$ (4). When disagreement is high, a positive $\bar{\kappa}$ would amplify unreliable targets, increasing the risk of overestimation. To prevent this, the learning objective in (6) drives $\bar{\kappa}$ toward more negative values, promoting conservatism under disagreement. In contrast, κ modulates the actor’s aggregation via \tilde{Q}_{κ} and is optimized to match $y_{\bar{\kappa}}$, which, as noted earlier, is typically larger than \tilde{Q}_{κ} . When disagreement δ is high, (7) discourages large κ values. As disagreement declines, κ has room to increase, allowing optimistic updates that encourage exploration. This interplay ensures DEA’s actor gradually becomes more explorative as disagreement diminishes. The evolution of κ and $\bar{\kappa}$ during training is illustrated in the next section and in Figure 1.

6 Experiments

Learning regimes The goal of our experiments is to evaluate DEA across learning settings that differ in sample efficiency and update frequency. These regimes are defined by the update-to-data (UTD) ratio, which specifies how many gradient updates are performed per environment interaction. We consider two regimes — interactive and sample-efficient — ranging from low to high update intensity. To align with each setting, we scale the ensemble size proportionally to the UTD ratio; smaller ensembles minimize compute in interactive settings, while larger ensembles promote stability when updates are frequent.

Table 2 summarizes the learning regimes. SAC is typically used for the interactive, while REDQ is designed for sample-efficient one. DEA is evaluated in both to assess its ability to generalize.

Evaluation metrics We evaluate performance using three standard metrics: Final return measures the average return at the end of training across evaluation repetitions; InterQuartile Mean (IQM) of the final evaluation-time return provides a robust average across seeds by excluding outliers [2]; Area Under the Learning Curve (AULC) captures the cumulative reward over the course of training, reflecting both speed and stability of learning. For each metric and environment, we assign a rank to each method, where a lower rank indicates better performance (i.e., rank 1 is best, rank 2 is second-best, and so on). The average rank is then computed across all environments for each metric.

Experimental setup We conduct experiments on continuous control tasks from the MuJoCo physics simulator [7, 38, 39, version v5], evaluating performance under multiple learning regimes that vary in sample efficiency and update frequency (see Table 2 for details). We selected them because the limitations of static aggregation and the benefits of adaptive strategies are already clearly pronounced in these settings, and we do not expect qualitatively different behavior in other continuous control tasks. All experiments are repeated across ten seeds. All methods use automatic entropy temperature tuning of α , as described in Haarnoja et al. [15]. A detailed overview of architecture, training settings, and hyperparameters is provided in Appendix B.

Learning trajectories of directional parameters $\bar{\kappa}$ and κ To better understand how DEA modulates aggregation during training, Figure 1 visualizes the trajectories of $\bar{\kappa}$ and κ under the two

Table 2: Learning regimes.

Learning regime	Ensemble size	Environment interactions	UTD ratio
Interactive	2	1.000.000	1
Sample-efficient	10	300.000	20

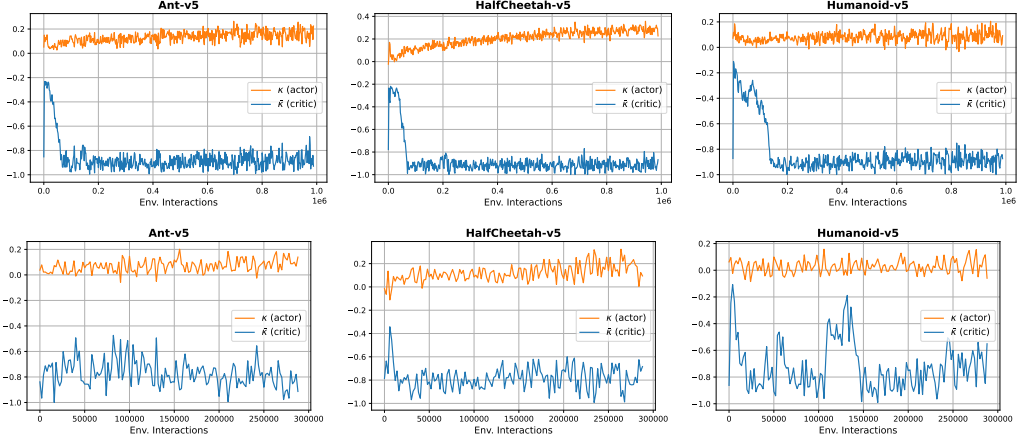


Figure 1: Trajectories of the directional aggregation parameters $\bar{\kappa}$ (critic) and κ (actor) on MuJoCo environments. The top row shows results for the interactive regime, and the bottom row for the sample-efficient regime (Table 2).

Table 3: Performance on MuJoCo env. aggregated across learning regimes (Table 2). Metrics are average final return, InterQuantile Mean (IQM) of the final return, and Area Under the Learning Curve (AULC) — averaged over learning regimes, evaluation repetitions and ten seeds. Average rank is computed per metric across environments. \uparrow indicates higher is better, while \downarrow indicates lower is better. Best performing algorithm per metric are **bold**. Detailed results for each learning regime are provided in Table 5.

Environment	Final Return (\uparrow)			IQM (\uparrow)			AULC (\uparrow)		
	DEA	REDQ	SAC	DEA	REDQ	SAC	DEA	REDQ	SAC
Ant-v5	4920	4278	2199	5226	4712	2583	2829	2249	1556
HalfCheetah-v5	10158	10065	8267	10334	10039	8250	7745	7682	6600
Hopper-v5	3376	2756	2526	3543	2835	2760	2780	2432	1891
Humanoid-v5	5073	4682	4832	5331	5338	5311	3315	2864	2857
Walker2d-v5	4425	4440	2989	4663	4564	2716	3111	3037	1963
Avg. Rank (\downarrow)	1.2	1.8	3.0	1.2	1.8	3.0	1.0	2.2	2.8

learning regimes (Table 2). We initialize the aggregation parameters as $\bar{\kappa} = -0.8$ and $\kappa = 0.0$; an ablation of initialization sensitivity is provided in Section 7. To ensure stable optimization in an unconstrained parameter space, we apply a tangent transformation to map both parameters into the open interval from minus one to one. The first row of the figure corresponds to the interactive regime, and the second row to the sample-efficient regime. The trends align with the behavior anticipated from our analysis in Section 5. In particular, as training progresses, $\bar{\kappa}$ typically remains negative, anchoring conservative critic estimates, while κ tends to be positive and further increases when learning proceeds, to support explorative actor behavior. This dynamic interplay reflects DEA’s ability to adaptively balance exploration and conservatism based on the ensemble disagreement and training context. Trajectories across all tasks, seeds, and learning regimes can be found in Appendix C.

Generalization across learning regimes Average performance across both learning regimes is summarized in Table 3; detailed results for each individual regime are provided in Table 5 (Appendix C). DEA consistently matches or outperforms the best-performing baseline across tasks and metrics. Notably, it achieves the highest average rank in all three metrics — final return, IQM, and AULC — with a particularly strong lead in AULC, indicating more reliable and efficient learning over time. Unlike existing methods, which are typically optimized for a fixed learning regime, DEA adapts its aggregation strategy during training — it adjusts the level of conservatism and optimism based on ensemble disagreement and training context — enabling it to generalize across learning regimes.

In particular, SAC is designed for low-UTD settings with small ensembles and often becomes overly conservative under higher UTD ratios. REDQ, by contrast, performs well in sample-efficient settings where its high UTD ratio and large ensemble size support rapid learning. Yet, REDQ tends to be unstable or less effective in low-update regimes, where its fixed update strategy becomes less reliable. DEA avoids these limitations by dynamically adjusting its behavior to the demands of the training context, rather than relying on static aggregation rules.

Learning curves and trajectories of the directional aggregation parameters ($\bar{\kappa}$ and κ) across all tasks and learning regimes are provided in Appendix C (Figures 2 to 5).

7 Ablations

Our experiments already spans two distinct learning regimes — interactive and sample-efficient — which naturally serve as ablations over ensemble size and UTD ratio. As shown in Section 6, DEA remains effective across these varying configurations.

Fixed aggregation and degenerate cases A natural ablation is to fix $\bar{\kappa}$ and κ to constants. Doing so effectively recovers existing baselines: for example, setting both to enforce a static minimum corresponds to the conservative update used in SAC, while using a fixed mean aligns with REDQ. These variants remove DEA’s adaptivity and result in behavior already covered by prior methods.

Fixing either $\bar{\kappa}$ or κ individually also degrades performance. As described in Section 5, these parameters act as directional anchors: $\bar{\kappa}$ controls critic-side conservatism, while κ guides actor-side aggregation. Learning both jointly is crucial to allow DEA to interpolate between exploration and caution based on ensemble disagreement. Without this flexibility, the critic and actor can become misaligned, undermining the value of directional ensemble learning. In such cases, DEA loses its ability to adapt to uncertainty and learning dynamics, and its performance suffers accordingly.

Sensitivity to initializations We study the sensitivity of DEA to different initializations of the critic-side aggregation parameter $\bar{\kappa}$, while keeping the actor-side initialization of κ fixed at zero. This isolates the effect of $\bar{\kappa}$ and avoids interactions between the two directional parameters. Initializing κ at zero provides a neutral initialization that does not bias the actor toward conservatism or optimism at the start of training. Results are shown in Figures 8 and 9 (Appendix D). As expected, the impact of initialization varies across tasks and learning regimes. While these results highlight the importance of choosing a good initialization — especially in higher UTD settings — DEA remains stable across all tested configurations, thanks to its robustness to the unforeseen effects of numerical perturbations. This robustness stems from its directional update rule, which only preserves the essential sign-information. None of the initializations lead to divergence or collapse, and many configurations outperform both SAC and REDQ.

8 Related work

Ensemble methods in off-policy RL have been widely studied for their ability to stabilize training, estimate uncertainty, and facilitate exploration. Below, we review prior work through three lenses most relevant to our work: (i) reducing overestimation bias, (ii) enabling efficient exploration, and (iii) improving sample efficiency across varying update-to-data (UTD) regimes. These objectives often overlap, and many methods address multiple goals simultaneously. Below, we highlight representative approaches within each category. A more detailed discussion is provided in Appendix A.

Reducing overestimation bias with ensembles Overestimation bias in Q -value estimates can destabilize training and degrade policy performance. To address this issue, various methods have been proposed for both discrete and continuous control. In discrete-action settings, overestimation is mitigated by aggregating multiple Q -value estimates in various different manners [4, 18, 40, 41]. However, these techniques do not extend naturally to continuous control. In continuous settings, TD3 [12] proposed taking the minimum over two Q -networks to reduce bias, a strategy adopted and extended by SAC [14] and others [10, 11]. These methods stabilize training by conservatively anchoring the target through fixed ensemble aggregation rules. DEA, on the other hand, avoids such hard-coded ensemble rules and allows adjusting ensembles dynamics based on training dynamics.

Recently, regularized value estimation methods have sought to adaptively reduce bias. GPL [8], for example, uses a distributional critic and dual TD-learning with regularization. However, GPL does not straightforwardly generalize outside its narrow learning regime — struggling in interactive (low-UTD) settings and requiring large ensembles and high UTD ratios for stability [8, Figures 13 and 15]. Its sample efficiency depends on pre-tuned, task-specific hyperparameters, particularly heuristic entropy targets, and a fixed optimism schedule [8, Tables 2 and 3]. In contrast, DEA avoids such rigidity by using scalar Q -values and learning aggregation weights directly from data, adapting flexibly across learning regimes without distributional modeling or handcrafted schedules.

Efficient exploration While conservative value estimates provide stability, they can suppress exploration and slow learning. Prior approaches for discrete control encourage exploration by leveraging ensemble disagreement [9, 30]. In continuous control, OAC [11] leverages upper confidence bounds to guide exploration, while TOP [25] frames the trade-off between conservatism and exploration as a multi-armed bandit problem, switching between predefined aggregation strategies. DAC [26] takes a different approach by maintaining two actors — a pessimistic one for conservative updates and an optimistic one for exploration. DEA differs from these methods by guiding a single actor through a fully learnable aggregation scheme. Rather than relying on handcrafted decision rules, confidence bounds, or architectural complexity, DEA integrates ensemble disagreement directly into the actor update and adjusts exploration adaptively during training.

Sample efficiency Improving sample efficiency is a central goal in off-policy RL. REDQ [10] addresses this by using large ensembles and high UTD ratios. However, REDQ relies on a fixed aggregation strategy and does not adapt to evolving uncertainty or training dynamics. AQE [43] and TQC [17] enhance learning by either averaging over subsets of multi-head critics (AQE) or truncating the highest Q -value estimates (TQC). However, both approaches require manually chosen thresholds or hyperparameters that must be tuned separately for each task or training regime. In contrast, DEA dynamically adapts its aggregation behavior based on ensemble disagreement, automatically adjusting conservatism and exploration without relying on fixed schedules or per-task tuning.

Other methods like SUNRISE [20] and MeanQ [21] also promote sample-efficient learning but are tailored to fixed schedules and architectures. DEA instead modulates ensemble aggregation dynamically, allowing a single actor-critic algorithm to perform robustly across both interactive (low-UTD) and sample-efficient (high-UTD) regimes without manual tuning.

DEA aims to learn a general-purpose aggregation mechanism that operates effectively across learning regimes — from interactive (low-UTD) to sample-efficient (high-UTD) settings — by leveraging ensemble disagreement in a principled, learnable manner. In this landscape, SAC [14] and REDQ [10] represent widely adopted baselines for interactive and sample-efficient learning, respectively.

9 Discussion

DEA is an adaptive ensemble-based method for actor-critics that works across learning regimes. Its key strength is adaptability: DEA learns directional aggregation weights that evolve with the data, allowing it to adjust autonomously to varying tasks, uncertainty levels, and training dynamics. This flexibility allows DEA to perform reliably across both interactive and sample-efficient settings — something that prior methods typically address only in isolation — without relying on heuristic aggregation rules, auxiliary actors, or handcrafted regularization.

Limitations Despite its strong empirical performance, DEA has several limitations. The introduction of learnable aggregation parameters adds complexity to the training process, making optimization more sensitive to initialization, hyperparameters, and ensemble calibration. While DEA remains stable across tasks and seeds in our experiments, its effectiveness may diminish in highly stochastic environments or when ensembles are too small to provide meaningful disagreement signals. Next, we deliberately focused on dense-reward environments where random exploration often suffices and the impact of estimation bias can be partially offset by existing heuristics. That DEA still demonstrates clear improvements in this setting underscores the strength of the approach; we expect these benefits to be even more pronounced in sparse-reward environments where exploration is more challenging. Although empirical results suggest that directional aggregation mitigates overestimation bias and improves learning, these benefits are not yet supported by theoretical analysis. A key challenge is

that DEA’s learnable aggregation rules depend on ensemble disagreement and the sign of Bellman errors, coupling the dynamics of the aggregation parameters with those of the actor and critic in a non-trivial way.

Future work Our work focuses exclusively on online RL; extending these ideas to the offline setting is an exciting direction for future work, especially building on the promising findings demonstrated in the online setting. Another avenue is evaluating DEA in sparse-reward environments, where adaptivity to uncertainty may be especially beneficial. Finally, pairing DEA with more advanced actor-critic frameworks — such as BRO [28] or Simba [19] — could further improve learning.

Acknowledgments and Disclosure of Funding

This work was supported by grants from the Novo Nordisk Foundation (NNF) under grant number NNF21OC0070621 and the Carlsberg Foundation (CF) under grant number CF21-0250.

References

- [1] Z. Abbas, R. Zhao, J. Modayil, A. White, and M. C. Machado. Loss of plasticity in continual deep reinforcement learning. In *Conference on Lifelong Learning Agents (CoLLAs)*, 2023.
- [2] R. Agarwal, M. Schwarzer, P. S. Castro, A. C. Courville, and M. Bellemare. Deep reinforcement learning at the edge of the statistical precipice. *Advances in Neural Information Processing Systems (NeurIPS)*, 2021.
- [3] G. An, S. Moon, J.-H. Kim, and H. O. Song. Uncertainty-based offline reinforcement learning with diversified q-ensemble. *Advances in Neural Information Processing Systems (NeurIPS)*, 2021.
- [4] O. Aenschel, N. Baram, and N. Shimkin. Averaged-dqn: Variance reduction and stabilization for deep reinforcement learning. In *Proceedings of the International Conference on Machine Learning (ICML)*, 2017.
- [5] M. G. Bellemare, W. Dabney, and M. Rowland. *Distributional reinforcement learning*. MIT Press, 2023.
- [6] D. Bertsekas and J. N. Tsitsiklis. *Neuro-dynamic programming*. Athena Scientific, 1996.
- [7] G. Brockman, V. Cheung, L. Pettersson, J. Schneider, J. Schulman, J. Tang, and W. Zaremba. OpenAI Gym. *arXiv preprint arXiv:1606.01540*, 2016.
- [8] E. Cetin and O. Celiktutan. Learning pessimism for reinforcement learning. In *Proceedings of the AAAI Conference on Artificial Intelligence*, 2023.
- [9] R. Y. Chen, S. Sidor, P. Abbeel, and J. Schulman. Ucb exploration via q-ensembles. *arXiv preprint arXiv:1706.01502*, 2017.
- [10] X. Chen, C. Wang, Z. Zhou, and K. W. Ross. Randomized ensembled double q-learning: Learning fast without a model. In *International Conference on Learning Representations (ICLR)*, 2021.
- [11] K. Ciosek, Q. Vuong, R. Loftin, and K. Hofmann. Better exploration with optimistic actor critic. *Advances in Neural Information Processing Systems (NeurIPS)*, 2019.
- [12] S. Fujimoto, H. Hoof, and D. Meger. Addressing function approximation error in actor-critic methods. In *Proceedings of the International Conference on Machine Learning (ICML)*, 2018.
- [13] T. Haarnoja, H. Tang, P. Abbeel, and S. Levine. Reinforcement learning with deep energy-based policies. In *Proceedings of the International Conference on Machine Learning (ICML)*, 2017.
- [14] T. Haarnoja, A. Zhou, P. Abbeel, and S. Levine. Soft actor-critic: Off-policy maximum entropy deep reinforcement learning with a stochastic actor. In *Proceedings of the International Conference on Machine Learning (ICML)*, 2018.
- [15] T. Haarnoja, A. Zhou, K. Hartikainen, G. Tucker, S. Ha, J. Tan, V. Kumar, H. Zhu, A. Gupta, P. Abbeel, et al. Soft actor-critic algorithms and applications. *arXiv preprint arXiv:1812.05905*, 2018.
- [16] D. Kingma and J. Ba. Adam: A method for stochastic optimization. In *International Conference on Learning Representations (ICLR)*, 2015.

- [17] A. Kuznetsov, P. Shvechikov, A. Grishin, and D. Vetrov. Controlling overestimation bias with truncated mixture of continuous distributional quantile critics. In *Proceedings of the International Conference on Machine Learning (ICML)*, 2020.
- [18] Q. Lan, Y. Pan, A. Fyshe, and M. White. Maxmin q-learning: Controlling the estimation bias of q-learning. In *International Conference on Learning Representations (ICLR)*, 2020.
- [19] H. Lee, D. Hwang, D. Kim, H. Kim, J. J. Tai, K. Subramanian, P. R. Wurman, J. Choo, P. Stone, and T. Seno. Simba: Simplicity bias for scaling up parameters in deep reinforcement learning. In *International Conference on Learning Representations (ICLR)*, 2025.
- [20] K. Lee, M. Laskin, A. Srinivas, and P. Abbeel. Sunrise: A simple unified framework for ensemble learning in deep reinforcement learning. In *Proceedings of the International Conference on Machine Learning (ICML)*, 2021.
- [21] L. Liang, Y. Xu, S. McAleer, D. Hu, A. Ihler, P. Abbeel, and R. Fox. Reducing variance in temporal-difference value estimation via ensemble of deep networks. In *Proceedings of the International Conference on Machine Learning (ICML)*, 2022.
- [22] T. Lillicrap, J. Hunt, A. Pritzel, N. Heess, T. Erez, Y. Tassa, D. Silver, and D. Wierstra. Continuous control with deep reinforcement learning. In *International Conference on Learning Representations (ICLR)*, 2016.
- [23] V. Mnih, K. Kavukcuoglu, D. Silver, A. Graves, I. Antonoglou, D. Wierstra, and M. Riedmiller. Playing atari with deep reinforcement learning. *arXiv preprint arXiv:1312.5602*, 2013.
- [24] V. Mnih, K. Kavukcuoglu, D. Silver, A. A. Rusu, J. Veness, M. G. Bellemare, A. Graves, M. Riedmiller, A. K. Fidjeland, G. Ostrovski, et al. Human-level control through deep reinforcement learning. *Nature*, 2015.
- [25] T. Moskovitz, J. Parker-Holder, A. Pacchiano, M. Arbel, and M. Jordan. Tactical optimism and pessimism for deep reinforcement learning. *Advances in Neural Information Processing Systems (NeurIPS)*, 2021.
- [26] M. Nauman and M. Cygan. Decoupled policy actor-critic: Bridging pessimism and risk awareness in reinforcement learning. In *Proceedings of the AAAI Conference on Artificial Intelligence*, 2025.
- [27] M. Nauman, M. Bortkiewicz, P. Miłoś, T. Trzcinski, M. Ostaszewski, and M. Cygan. Overestimation, overfitting, and plasticity in actor-critic: the bitter lesson of reinforcement learning. In *Proceedings of the International Conference on Machine Learning (ICML)*, 2024.
- [28] M. Nauman, M. Ostaszewski, K. Jankowski, P. Miłoś, and M. Cygan. Bigger, regularized, optimistic: scaling for compute and sample efficient continuous control. *Advances in Neural Information Processing Systems (NeurIPS)*, 2024.
- [29] E. Nikishin, M. Schwarzer, P. D’Oro, P.-L. Bacon, and A. Courville. The primacy bias in deep reinforcement learning. In *Proceedings of the International Conference on Machine Learning (ICML)*, 2022.
- [30] I. Osband, C. Blundell, A. Pritzel, and B. Van Roy. Deep exploration via bootstrapped dqn. *Advances in Neural Information Processing Systems (NeurIPS)*, 2016.
- [31] A. Paszke, S. Gross, F. Massa, A. Lerer, J. Bradbury, G. Chanan, T. Killeen, Z. Lin, N. Gimelshein, L. Antiga, A. Desmaison, A. Kopf, E. Yang, Z. DeVito, M. Raison, A. Tejani, S. Chilamkurthy, B. Steiner, L. Fang, J. Bai, and S. Chintala. PyTorch: An Imperative Style, High-Performance Deep Learning Library. *Advances in Neural Information Processing Systems (NeurIPS)*, 2019.
- [32] M. L. Puterman. *Markov decision processes: discrete stochastic dynamic programming*. John Wiley & Sons, 2014.
- [33] W. Shang, K. Sohn, D. Almeida, and H. Lee. Understanding and improving convolutional neural networks via concatenated rectified linear units. In *Proceedings of the International Conference on Machine Learning (ICML)*, 2016.
- [34] H. Sheikh, M. Phiellipp, and L. Boloni. Maximizing ensemble diversity in deep reinforcement learning. In *International Conference on Learning Representations (ICLR)*, 2022.
- [35] D. Silver, G. Lever, N. Heess, T. Degris, D. Wierstra, and M. Riedmiller. Deterministic policy gradient algorithms. In *Proceedings of the International Conference on Machine Learning (ICML)*, 2014.
- [36] R. S. Sutton and A. G. Barto. *Reinforcement learning: An introduction*. MIT Press, 2018.

- [37] S. Thrun and A. Schwartz. Issues in using function approximation for reinforcement learning. In *Proceedings of the Fourth Connectionist Models Summer School*, 1993.
- [38] E. Todorov, T. Erez, and Y. Tassa. Mujoco: A physics engine for model-based control. In *IEEE/RSJ International Conference on Intelligent Robots and Systems (IROS)*, 2012.
- [39] M. Towers, A. Kwiatkowski, J. Terry, J. U. Balis, G. De Cola, T. Deleu, M. Goulao, A. Kallinteris, M. Krimmel, A. KG, et al. Gymnasium: A standard interface for reinforcement learning environments. *arXiv preprint arXiv:2407.17032*, 2024.
- [40] H. Van Hasselt. Double q-learning. *Advances in Neural Information Processing Systems (NeurIPS)*, 2010.
- [41] H. Van Hasselt, A. Guez, and D. Silver. Deep reinforcement learning with double q-learning. In *Proceedings of the AAAI Conference on Artificial Intelligence*, 2016.
- [42] C. J. Watkins and P. Dayan. Q-learning. *Machine Learning*, 1992.
- [43] Y. Wu, X. Chen, C. Wang, Y. Zhang, and K. W. Ross. Aggressive q-learning with ensembles: Achieving both high sample efficiency and high asymptotic performance. *Advances in Neural Information Processing Systems (NeurIPS)*, 2022. Deep Reinforcement Learning Workshop.
- [44] B. D. Ziebart. *Modeling purposeful adaptive behavior with the principle of maximum causal entropy*. Carnegie Mellon University, 2010.

A Extended discussion of related work

Reducing overestimation bias with ensembles Overestimation bias in Q -value estimates can destabilize training and degrade policy performance. To address this issue, various methods have been proposed for both discrete and continuous control. In discrete-action settings, overestimation is mitigated by conservatively aggregating multiple Q -value estimates, as in Double Q -learning [40, 41], Averaged DQN [4], and Maxmin Q -learning [18]. However, these techniques do not extend naturally to continuous control.

In continuous settings, TD3 [12] proposed taking the minimum over two Q -networks to reduce bias, a strategy adopted and extended by SAC [14] and others [10, 11]. These methods stabilize training by conservatively anchoring the target through fixed ensemble aggregation rules. DEA generalizes these approaches by introducing learnable, directional aggregation parameters for the critic and the actor, enabling adaptive control over conservatism and exploration in response to ensemble disagreement.

Recently, regularized value estimation methods have also sought to address bias adaptively. GPL [8], for example, introduces a regularization mechanism based on a distributional critic and dual TD-learning. While it can be effective in specific settings, GPL performs poorly outside its narrow operating regime – struggling in interactive learning scenarios and relying heavily on large ensembles and high UTD ratios for stability and performance [8, Figures 13 and 15]. Moreover, its apparent sample efficiency depends on extensive pre-tuning; it requires task-specific hyperparameters, particularly heuristic entropy targets that are carefully selected for each environment [8, Tables 2]. Another limitation of GPL is its reliance on a deterministic optimism schedule that forces the actor to behave optimistically early in training and gradually shift toward conservatism [8, Tables 3]. In contrast, DEA avoids such rigidity. DEA uses standard scalar Q -values and learns both actor- and critic-side aggregation weights directly from data, adapting flexibly across learning regimes without relying on distributional modeling, fixed optimism schedules, or heuristic entropy targets.

Efficient exploration While conservative value estimates provide stability, they can suppress exploration and slow learning. To encourage exploration, several ensemble-based strategies have been developed. In discrete-action settings, Bootstrapped DQN [30] and its UCB-based extension [9] use ensemble disagreement to approximate posterior uncertainty and enable Thompson sampling.

In continuous control, OAC [11] leverages upper confidence bounds to guide exploration, while TOP [25] frames the trade-off between conservatism and exploration as a multi-armed bandit problem, switching between predefined aggregation strategies. DAC [26] takes a different approach by maintaining two actors – a pessimistic one for conservative updates and an optimistic one for exploration. DEA differs from these methods by guiding a single actor through a fully learnable aggregation scheme. Rather than relying on handcrafted decision rules, confidence bounds, or

architectural complexity, DEA integrates ensemble disagreement directly into the actor update and adjusts exploration adaptively during training.

Sample efficiency Improving sample efficiency is a central goal in off-policy RL. REDQ [10] addresses this by using large ensembles and high UTD ratios. However, REDQ relies on a fixed aggregation strategy and does not adapt to evolving uncertainty or training dynamics. AQE [43] and TQC [17] enhance learning by either averaging over subsets of multi-head critics (AQE) or truncating the highest Q -value estimates (TQC). However, both approaches require manually chosen thresholds or hyperparameters that must be tuned separately for each task or training regime. In contrast, DEA dynamically adapts its aggregation behavior based on ensemble disagreement, automatically adjusting conservatism and exploration without relying on fixed schedules or per-task tuning.

Other methods, such as SUNRISE [20] and MeanQ [21], also target sample-efficient learning but are tailored to fixed regimes and require specific aggregation strategies. While some Q -learning-based methods like Maxmin Q -learning [18] and Average DQN [4] offer insights into efficient learning, they focus on discrete control and are less applicable to continuous domains. In contrast, DEA modulates ensemble aggregation dynamically, allowing a single actor-critic algorithm to perform robustly across both interactive (low-UTD) and sample-efficient (high-UTD) regimes without manual tuning.

Ensemble disagreement and diversity Additional ensemble-based methods leverage disagreement or diversity as a regularization signal. MED-RL [34] uses diversified ensemble for RL. However, it is different from DEA in at least two ways: (i) the diversity is measured on the representation of the networks, not the Q -value itself, and (ii) the diversity is used as a regularizer that can be incorporated into existing algorithms. In contrast, DEA focuses on value-level disagreement and learns to modulate aggregation weights directly, with no algorithm-specific dependencies or architectural overhead.

In offline RL, where overestimation and distributional shift are particularly pronounced, ensembles are used to induce conservative value estimates. EDAC [3], for instance, leverage ensembles to detect out-of-distribution actions and penalize them. These methods assume a fixed dataset and often require very large ensembles (e.g., 50+ critics). Moreover, their use of ensemble disagreement is limited to regularizing critic training, while both the target Q -value and actor updates still rely on the minimum of the ensemble. DEA shares the conservatism goal but is designed for online RL and avoids such structural burdens by learning adaptive aggregation parameters that regulate the influence of ensemble disagreement over time.

B Experimental setup, hyperparameters, and implementation details

Our experiments are implemented in PyTorch [31, Version 2.1.0]. We conduct experiments on continuous control tasks using the v5-versions of the MuJoCo physics engine [7, 38, 39].

The specific ensemble sizes, number of environment interactions, and update-to-data (UTD) ratios used in each learning regime are shared across all methods, and are detailed in Table 2.

The hyperparameters used in our experiments are summarized in Table 4. These configurations follow the original implementations of SAC [14] and REDQ [10]. Following the recommendations of Nauman et al. [27], we use Concatenated ReLU (CReLU) activations to prevent the loss of plasticity in deep RL networks [1, 33].

As outlined in Section 2, all soft actor-critic methods learn the entropy temperature α dynamically using the method proposed in Haarnoja et al. [15], which tunes α to match a target entropy based on the action dimensionality; see Table 4 for specific values.

Table 4: Model architectures and hyperparameters shared across DEA, REDQ, and SAC.

Hyperparameter	DEA	REDQ	SAC
<i>Network architecture (actor and critics)</i>			
Hidden layers		2	
Layer size		256	
Activation function		CReLU	
<i>Optimization</i>			
Batch size	256		
Optimizer		Adam [16]	
Learning rate	$3 \cdot 10^{-4}$		
<i>General training configuration</i>			
Replay buffer size	$1 \cdot 10^6$		
Random initial steps	10,000		
Discount factor (γ)	0.99		
Target smoothing (τ)	$5 \cdot 10^{-3}$		
Initial entropy (α)	0.2		
Target entropy ($\mathcal{H}_{\text{target}}$)	$-\dim(\mathcal{A})/2$		
Seeds	{1, 2, ..., 10}		

Table 5: Performance on MuJoCo environments across learning regimes (Table 2). Metrics are average final return, InterQuantile Mean (IQM) of the final return, and Area Under the Learning Curve (AULC) — averaged over evaluation repetitions and ten seeds. \pm denotes standard deviation over seeds. Average rank is computed per metric across environments. \uparrow indicates higher is better, while \downarrow indicates lower is better.

Interactive learning (1M env. interactions, 2 critics, 1 update-to-data ratio)									
Environment	Final Return (\uparrow)			IQM (\uparrow)			AULC (\uparrow)		
	DEA	REDQ	SAC	DEA	REDQ	SAC	DEA	REDQ	SAC
Ant-v5	5355 \pm 1126	4083 \pm 1477	4396 \pm 1911	5708 \pm 200	4595 \pm 451	5164 \pm 502	3292	2168	3052
HalfCheetah-v5	10595 \pm 947	11437 \pm 264	10947 \pm 630	11007 \pm 70	11400 \pm 80	11074 \pm 138	8423	8791	8533
Hopper-v5	3425 \pm 379	2344 \pm 842	3060 \pm 885	3531 \pm 22	2254 \pm 538	3458 \pm 80	2901	2097	2482
Humanoid-v5	4780 \pm 1295	4646 \pm 1420	4761 \pm 1225	5286 \pm 35	5271 \pm 360	5281 \pm 102	3689	2734	3346
Walker2d-v5	4270 \pm 1350	4182 \pm 1352	4396 \pm 245	4674 \pm 155	4378 \pm 246	4396 \pm 108	3273	2749	2962
Avg. Rank (\downarrow)	1.6	2.6	1.8	1.4	2.6	2.0	1.4	2.6	2.0

Sample-efficient learning (300K env. interactions, 10 critics, 20 update-to-data ratio)									
Environment	Final Return (\uparrow)			IQM (\uparrow)			AULC (\uparrow)		
	DEA	REDQ	SAC	DEA	REDQ	SAC	DEA	REDQ	SAC
Ant-v5	4485 \pm 1044	4473 \pm 1142	1 \pm 4	4744 \pm 260	4828 \pm 398	1 \pm 1	2367	2329	61
HalfCheetah-v5	9721 \pm 817	8692 \pm 1380	5586 \pm 662	9661 \pm 395	8678 \pm 813	5425 \pm 191	7066	6573	4666
Hopper-v5	3326 \pm 583	3169 \pm 592	1992 \pm 1278	3555 \pm 32	3415 \pm 153	2063 \pm 1034	2659	2766	1300
Humanoid-v5	5365 \pm 446	4718 \pm 1544	4903 \pm 1376	5376 \pm 87	5404 \pm 61	5341 \pm 124	2941	2994	2368
Walker2d-v5	4579 \pm 815	4697 \pm 599	1581 \pm 1384	4652 \pm 267	4749 \pm 170	1035 \pm 830	2949	3325	964
Avg. Rank (\downarrow)	1.2	2.0	2.8	1.6	1.4	3.0	1.6	1.4	3.0

Across all learning regimes (Table 2), we use the same network architecture, batch sizes, and learning rates to ensure comparability. The overall compute cost is similar across SAC, REDQ, and DEA when the number of critics and update-to-data ratios are matched.

The DEA method introduces only a negligible computational overhead due to the additional scalars κ and $\bar{\kappa}$ and their gradients. All experiments were run on NVIDIA GeForce RTX 4090 GPUs. Four seeds were run in parallel, resulting in a wall-clock time of approximately 3–8 hours to complete all four seeds, depending on the environment and learning regime (Table 2). The full DEA learning procedure is summarized in Algorithm 1.

C Additional experimental results

This appendix provides additional experimental results for all MuJoCo environments across the two learning regimes defined in Table 2.

Results in each learning regime Table 5 presents performance metrics for DEA, REDQ, and SAC across five MuJoCo environments under two learning regimes.

In the interactive regime, DEA consistently achieves the best or near-best scores across all environments. It obtains the best ranks for all metrics, outperforming both SAC and REDQ. SAC remains competitive in this regime, benefiting from its simplicity and robust performance with small ensembles. REDQ, on the other hand, performs worse — likely due to its on acting on the mean of the Q -values. DEA’s strong performance under these constraints suggests that its directional aggregation mechanism adapts well.

In the sample-efficient regime, results are more nuanced. DEA achieves the best average rank in final return but not in IQM or AULC, where REDQ slightly edges ahead. DEA still maintains strong overall performance and outperforms SAC by a wide margin. REDQ benefits from the increased update frequency and larger ensemble, improving its scores in this regime. While REDQ ranks highest in IQM and AULC, DEA is overall on-par.

Overall, these results show that DEA performs competitively across regimes, offering both adaptability and stability, though REDQ may have an edge in the sample-efficient setting. For a summarized cross-regime comparison, including aggregated metrics and average ranks, see Table 3.

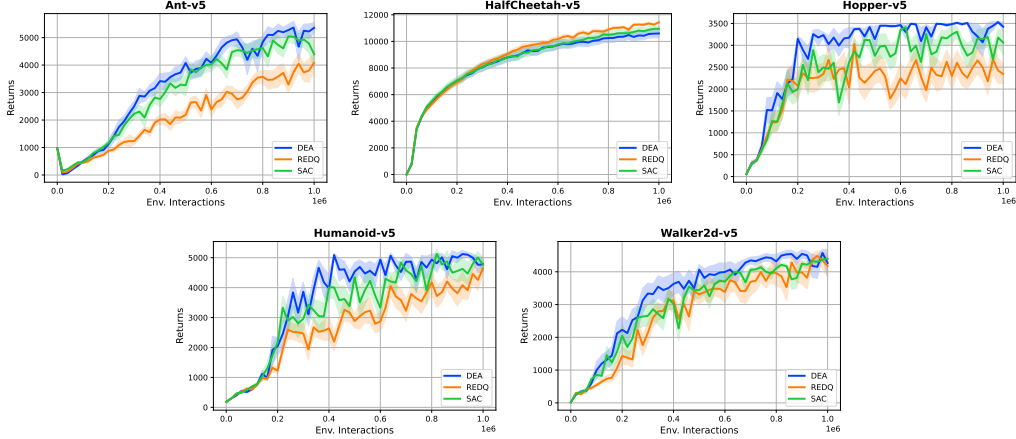


Figure 2: Learning curves for all MuJoCo tasks under the interactive learning regime (Table 2). Results are averaged over ten seeds, with shaded regions indicating one standard deviation.

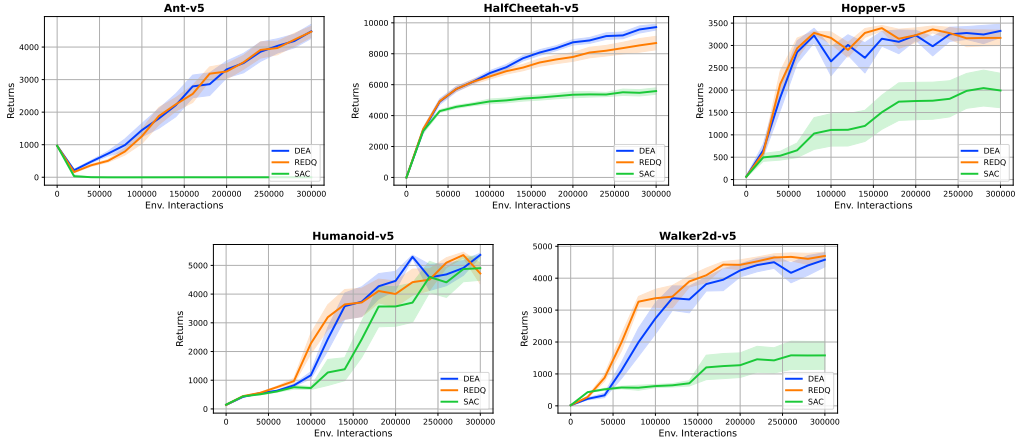


Figure 3: Learning curves for all MuJoCo tasks under the sample-efficient learning regime (Table 2). Results are averaged over ten seeds, with shaded regions indicating one standard deviation.

Learning curves Figures 2 and 3 show the full learning curves for all tasks under the interactive and sample-efficient learning regimes, respectively. Results are averaged over ten seeds, and shaded regions correspond to one standard deviation.

DEA generally outperforms SAC and REDQ in their respective learning regimes. In the interactive regime, SAC remains competitive due to its simplicity and stability with small ensembles. However, as ensemble size and update frequency increase, its static conservative aggregation becomes overly restrictive, limiting both learning speed and final performance. Conversely, REDQ performs well in sample-efficient settings, where its high UTD ratio and large ensemble size support rapid learning — but it becomes less reliable in low-update regimes. DEA bridges this gap by learning to adjust its aggregation strategy dynamically based on ensemble disagreement and training context, achieving stable and robust performance across both regimes. Notably, DEA overall achieves top ranks, highlighting its effectiveness in learning under different UTD ratios and ensemble sizes.

Directional aggregation trajectories Figures 4 and 5 show the evolution of the learned directional aggregation parameters ($\bar{\kappa}$ for the critic and κ for the actor) throughout training across the two learning regimes for each of the seeds. These figures illustrate how DEA adjusts aggregation behavior in response to training dynamics. $\bar{\kappa}$ typically remains negative, anchoring conservative critic estimates, while κ tends to increase, supporting more explorative actor behavior.

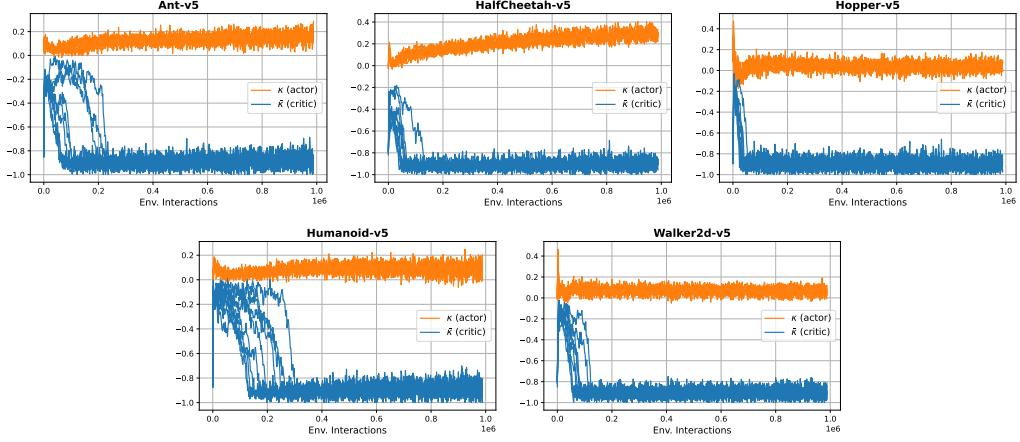


Figure 4: Trajectories of the directional aggregation parameters $\bar{\kappa}$ (critic) and κ (actor) across seeds in MuJoCo environments under the interactive learning regime (Table 2).

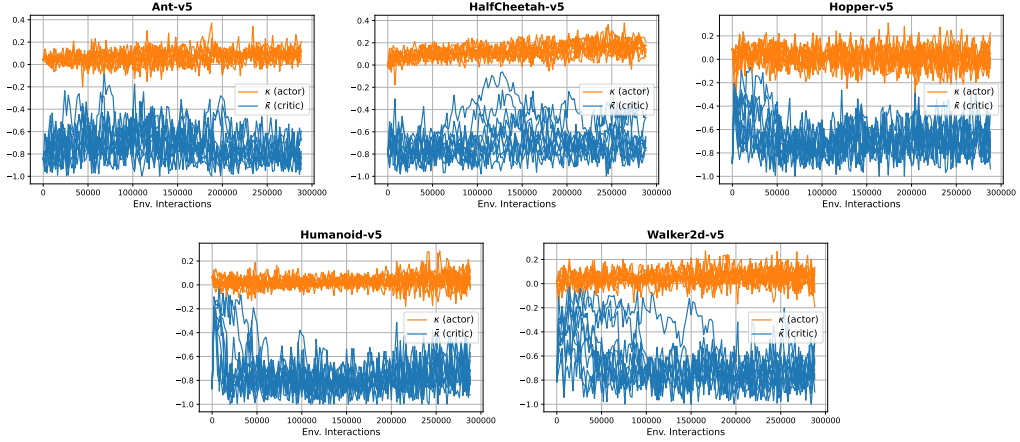


Figure 5: Trajectories of the directional aggregation parameters $\bar{\kappa}$ (critic) and κ (actor) across seeds in MuJoCo environments under the sample-efficient learning regime (Table 2).

Ensemble disagreement trajectories Figures 6 and 7 show the evolution of ensemble disagreement in the critic throughout training across both learning regimes. Early in training, limited data and untrained critics result in high disagreement across the ensemble. As training progresses and the critics become more aligned, disagreement generally decreases – particularly when measured relative to the increasing scale of the Q -values.

D Ablation details

This appendix provides additional results for the ablation study on the initialization of the directional aggregation parameters, as discussed in Section 7. Specifically, we investigate the effect of different initial values for the critic-side parameter $\bar{\kappa}$ while keeping the actor-side parameter fixed at $\kappa = 0$. This setup isolates the influence of $\bar{\kappa}$ on learning performance and avoids confounding interactions between the two parameters.

All results presented in this section are based on a single seed (seed 1). The purpose of this ablation is not to assess overall performance but to explore the stability and qualitative behavior of DEA under varying initializations.

Figures 8 and 9 shows learning curves across MuJoCo environments in the two learning regimes, respectively. Each subplot compares DEA’s performance under different $\bar{\kappa}$ initializations, including

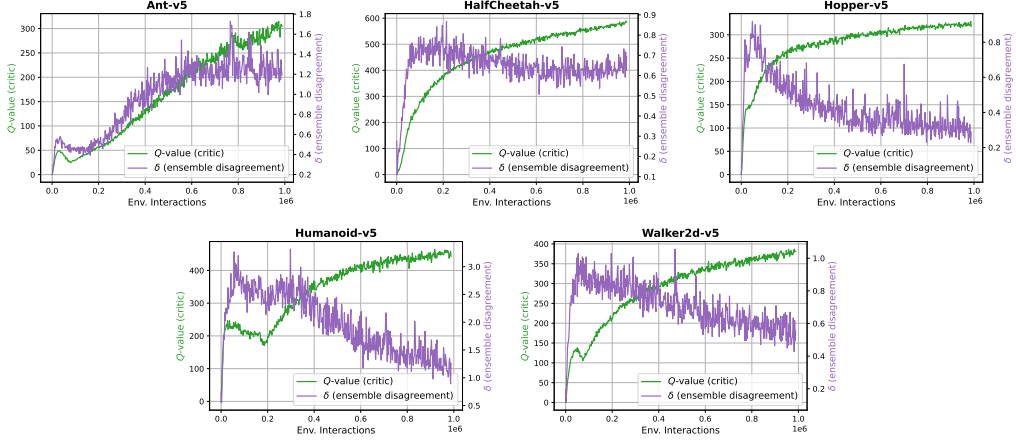


Figure 6: Trajectories of the directional aggregation parameters $\bar{\kappa}$ (critic) and κ (actor) across seeds in MuJoCo environments under the interactive learning regime (Table 2).

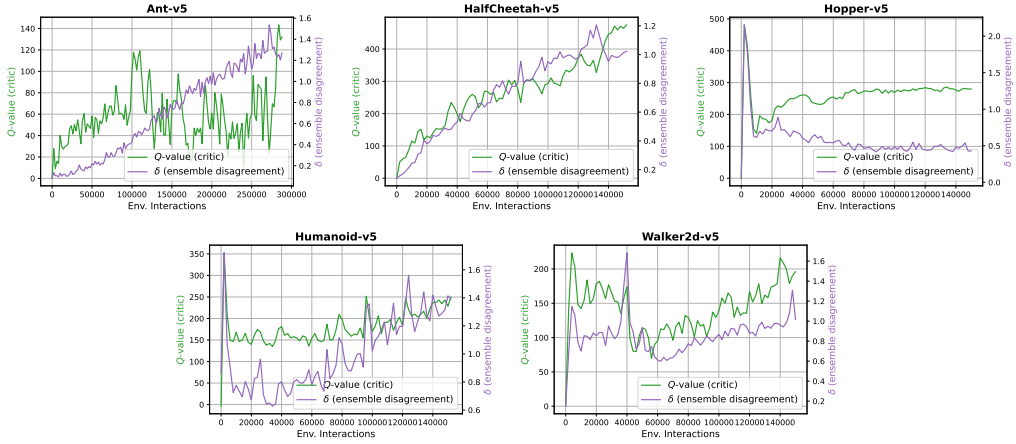


Figure 7: Trajectories of the directional aggregation parameters $\bar{\kappa}$ (critic) and κ (actor) across seeds in MuJoCo environments under the sample-efficient learning regime (Table 2).

SAC and REDQ. As discussed in Section 7, initialization has a more pronounced effect in high-UTD settings, where early updates to $\bar{\kappa}$ occur before new data is collected. Nevertheless, DEA remains stable across all settings, and in many instances still outperforms SAC and REDQ.

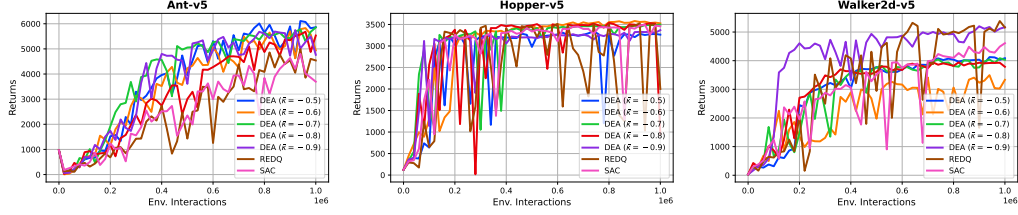


Figure 8: Effect of initializing the critic-side directional aggregation parameter $\bar{\kappa}$ on DEA’s performance across MuJoCo environments under the interactive learning regime (Table 2).

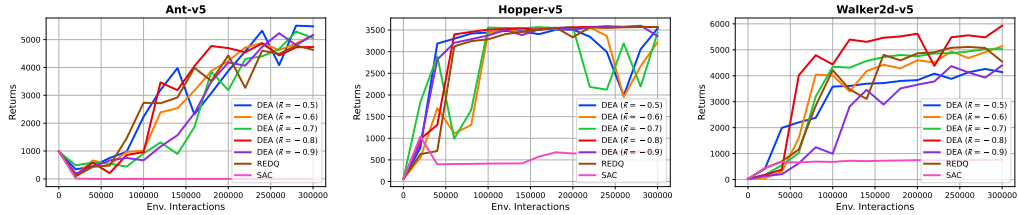


Figure 9: Effect of initializing the critic-side directional aggregation parameter $\bar{\kappa}$ on DEA’s performance across MuJoCo environments under the sample-efficient learning regime (Table 2).